



## PMN Apoptosis Induced by SNHG11 through the Inhibition of Endotoxin-induced Acute Lung Injury NF-κB Pathway

Wenhui Hu<sup>#</sup>, Yaping Ying<sup>#</sup>, Lihong Jin, Lingling Chen, Tingmin Zhou, Xiaohong Jin\*

Taizhou Hospital of Zhejiang Province Affiliated to Wenzhou Medical University, Linhai, 317000, China

<sup>#</sup>These authors contributed equally to this work as co-first author

### ARTICLE INFO

#### Original paper

#### Article history:

Received: September 24, 2021

Accepted: December 14, 2021

Published: February 28, 2022

#### Keywords:

ALI, Snhg11, NF-κB Pathway, PMN, Endotoxin

### ABSTRACT

To investigate the impacts of small nucleolar RNA host gene 11 (SNHG11) on nuclear factor kappa-B (NF-κB) pathway and polymorphonuclear granulocyte (PMN) apoptosis in rats with endotoxin-induced acute lung injury (ALI). Forty rats were the experimental subjects. They were randomly grouped as a control group (Group C), an endotoxin group (Group E), an inhibitor group (Group I), and an activator group (Group A), with 10 rats in each group. The endotoxin-induced ALI rat model was built. Arterial Blood Gas Test (ABGT) was performed, and the Wet/Dry (W/D) ratio of lung weight was determined. The pathological variations in rat pulmonary tissues were scrutinized and scored. PMN in peripheral blood was isolated; its apoptosis was assessed, and its total NF-κB p65 and p-NF-κB p65 expressions were assessed. The expression of SNHG11 mRNA in pulmonary tissues was assessed. Results: Compared to Group C, the W/D ratios and pathological scores of Group E, Group I, and Group A boosted notably ( $P < 0.05$ ), while their ABGT indicators and PMN apoptosis rates dropped ( $P < 0.05$ ). Compared to Group E and Group I, the W/D ratio and pathological score of Group A dropped notably ( $P < 0.05$ ), while its ABGT indicators and PMN apoptosis rate boosted ( $P < 0.05$ ). Compared to Group C, the p-NF-κB p65 and SNHG11 expressions were boosted in Group E, Group I, and Group A ( $P < 0.05$ ); compared to Group E and Group I, the p-NF-κB p65 and SNHG11 expressions in Group A dropped ( $P < 0.05$ ). SNHG11 could relieve endotoxin-induced ALI, which might be associated with the acceleration of PMN apoptosis and the inhibition of the NF-κB pathway.

DOI: <http://dx.doi.org/10.14715/cmb/2022.68.2.21>

Copyright: © 2022 by the C.M.B. Association. All rights reserved.



### Introduction

Clinically, acute lung injury (ALI) is a common and critical disease of the respiratory system, which is mostly manifested as hypoxemia that is difficult to treat. Its pathogenesis is complex, its condition is dangerous, its prognosis is poor, and its mortality rate is high, bringing a heavy burden to society and patients (1). Therefore, the prevention and treatment of ALI have critical clinical worth. At present, for the pathogenesis of ALI, inflammatory response and apoptosis are research hot spots. Polymorphonuclear granulocyte (PMN) is an important inflammatory cell that causes the excessive inflammatory response of ALI. The activation of nuclear factor kappa-B (NF-κB) is also the initial link that controls the expression of many inflammatory mediators in inflammatory cells, which is vital for the activation of PMN (2). Research has shown that the gene expression of pro-inflammatory factors is regulated by the transcription mechanism; as a critical transcription factor, NF-κB is

vital to the pathogenesis of ALI (3). Research by Lv et al. (2016) showed that the serum lipopolysaccharide (LPS) in patients after trauma and surgeries boosted notably, activating the NF-κB (4). Zamoshnikova et al. (2016) reported that the production of cytokines when NF-κB was activated would activate NF-κB in turn, causing a waterfall-like cascade of inflammatory cytokines; such a vicious cycle would aggravate the post-traumatic inflammatory responses (5). Therefore, controlling the expression of NF-κB during LPS activation is helpful for the regulation of postoperative inflammatory cytokines.

Research by Luo et al. (2020) showed that small nucleolar RNA host gene 11 (SNHG11) was highly expressed in the pulmonary tissue of ALI (6). At present, SNHG11 has been found to be highly expressed in some tumors (7-9). However, reports on SNHG11 expressed in ALI are none. Therefore, it is necessary to analyze the impacts of SNHG11 on the development of ALI diseases, thereby laying the

\*Corresponding author. E-mail: [renpo624958944223@163.com](mailto:renpo624958944223@163.com)  
Cellular and Molecular Biology, 2022, 68(2): 145-152

foundation for finding new therapeutic targets for ALI.

To clarify the role of SNHG11 in the NF- $\kappa$ B pathway and PMN, the Sprague-Dawley (SD) rats were utilized to explore the impacts of SNHG11 on the NF- $\kappa$ B pathway and PMN apoptosis in rats with endotoxin-induced ALI. The results would provide an experimental basis for the development and application of SNHG11, which had great worth.

## Materials and Methods

### Experimental Animal and Grouping

Forty clean-level SD rats (XXX animal center), aging 10 weeks and weighing about 200g, were purchased, among which the male-female ratio was 1:1. All rats were kept in separate cages and fed with national standard rodent feeds. 4 rats shared 1 cage, and could eat and drink freely. No significant differences were found in body weight between groups. All rats were given natural illumination and free diets. The room temperature was controlled at 20-26°C, humidity at 40-50%. The adaptive feeding continued for 2 weeks. The processes of animals and the experimental procedures were conducted in conformity with the *Chinese Experimental Animal Protection and Management Regulations* and were submitted to the approval of the superior ethics committee.

Rats were randomly grouped into a control group (Group C), an endotoxin group (Group E), an inhibitor group (Group I), and an activator group (Group A), with 10 rats in each group.

### Construction of Endotoxin-Induced ALI Rat Model

The ALI model was built by injecting LPS through the caudal vein. The tail of the rat was pulled out; the bristles at 2/3 of the tail root were removed, and the exposed skin was wiped repeatedly with an alcohol cotton ball until the veins were full. At a suitable location, the syringe was pierced along the vein, and blood being drawn back indicated that the puncture was successful. Rats in Group C were given 0.5 mL saline. Rats in Group E were given 0.5 mL LPS (5 mg/kg, Beijing Chreagen Biotechnology, China). Rats in Group I were given 0.5 mL LPS from the caudal veins and 0.5 mL SNHG11 inhibitor (1  $\mu$ g/kg, Shanghai Goybio, China) from the right abdomens.

Rats in Group A were given 0.5 mL LPS from the caudal veins and 0.5 mL SNHG11 activator (50 mg/kg, Shanghai Goybio, China) from the right abdomens. The injections shall be slow. Afterward, compression hemostasis was performed with aseptic cotton swabs.

### Sample Collection and Processing

Twenty-four hours after model construction, the samples were collected. Rat was anesthetized by intraperitoneal injection of chloral hydrate (10%, Beijing Solarbio Science & Technology, China). After anesthesia came into effect, the rat was fixed on a flat fixator (Beijing Heli Kechuang, China), with its abdomen pointing up. Then, its abdominal cavity was cut open to expose the abdominal aorta; 2 mL of blood was sampled with a blood sample collector and stored in a glycinate blood sample collection tube. All collected blood samples underwent Arterial Blood Gas Test (ABGT). Continuously, the arterial blood of rats was sampled. These blood samples were centrifuged (4000 r/min, 4°C) to collect the rat serum samples, which were stored at -70°C for flow cytometry and Western Blot. For each rat, its left pulmonary tissue was cut, stained with Hematoxylin-Eosin (HE), and tested by Reverse Transcription-Polymerase Chain Reaction (RT-PCR); its intact right lung was used for the determination of Wet/Dry (W/D) ratio.

### ABGT and Determination of Pulmonary W/D Ratio

After the blood samples were obtained, they were immediately analyzed by a blood gas analyzer. The PaO<sub>2</sub> and PaCO<sub>2</sub> values were measured and recorded, and the oxygenation index PaO<sub>2</sub>/FiO<sub>2</sub> was calculated.

The intact right lung was washed with saline and dried by an aseptic wiper. Its wet weight was determined by an electronic balance. Then, the lung was baked at 80°C for 24 h until its weight was constant. Its dry weight was determined, and the pulmonary W/D ratio was calculated.

### Observation of Pathological Variations in Pulmonary Tissues by HIM Staining

The pulmonary tissue samples were fixed with neutral formalin (10%, Wuhan Boster Biotechnology

Corporation, China); 48 h later, they were dehydrated by conventional gradient alcohol and cleared by xylene (Shenzhen Simeiquan Biotechnology, China). Then, the samples were embedded in conventional paraffin, washed with running water, and consecutively sectioned as 4 $\mu$ m-thick by an automatic tissue section (Shanghai Yuyanbio, China). The tissue sections were soaked in xylene and dewaxed for 5 min. This operation was repeated once. Then, the tissue sections were dehydrated by conventional gradient alcohol. After dehydration, the sections were stained with hematoxylin (Shanghai Zhengmao Biological Technology, China) for 15 min. The background shall not be too dark. The staining solution was rinsed with double-distilled water, and the sections were counter-stained by 1% hydrochloric acid alcohol for 3 min. When the nucleus and nucleus were clear, the staining was terminated. The sections were washed with double-distilled water for 20 min. Then, they were alkalized in lithium carbonate saturated solution (Shanghai Mengya Biotechnology, China) for 2 min. The distilled water around the sections was dried by an aseptic wiper. Then, they were stained with eosin (Beijing Dingguo Changsheng Biotechnology, China) for 3 min. After gradient alcohol dehydration and xylene clearing, the sections were sealed by neutral gum (Shanghai Yantuo Biological Technology, China). The pathological variations in pulmonary tissues were scrutinized and photographed by an optical microscope (Leica, Germany).

Besides, pathological scoring of pulmonary tissues was performed. The scoring items included pulmonary interstitial edema, alveolar edema, inflammatory cell infiltration, alveolar hemorrhage, hyaline membrane formation, and atelectasis. The scoring criteria were as follows: (1) 0 points: the lung interstitium, pulmonary blood vessels, alveoli, and bronchi were normal and without losses. (2) 1 point: a small amount of neutral white blood cells (WBCs) were seen in the interstitium, the interstitium and alveoli were bleeding, and the area of edema accounted for less than 25% of the lesion. (3) 2 points: more neutral WBCs were seen in the interstitium and part of the alveolar cavity, the interstitium was widened, with capillary congestion, and the hemorrhage and edema of the alveolar cavity accounted for 25% to 50% of the lesion. (4) 3 points:

aggregated WBCs existed in most alveoli and interstitium, the interstitium was notably widened, and the hemorrhage and edema of alveoli accounted for 50% to 75% of the lesion. (4) 4 points: the lesions filled the entire visual field. The score of total lung injury was the sum of the above items. For each rat, 10 400-time visual fields were scrutinized, and the score of each visual field was averaged.

#### **Isolation of Peripheral Blood PMN**

20 mL blood sample of each rat was anti-coagulated by heparin, added with 1:1 Hank's solution (Wuhan Chundubio, China), and mixed evenly. Then, the well-mixed sample was carefully dripped onto the surface of 40 mL rat PMN isolator (Tianjin Haoyang Biological Products, China) and centrifuged (666 g) for 15 min. Cells between Hank's solution and cell isolator were collected, whose red blood cells and plasma were removed. Then, the sample was put into a test tube with 5 mL of Hank's solution. After being mixed evenly, the sample was centrifuged (666g) for 15 min. The supernatant liquid was disposed of. The sample was washed and precipitated twice with Hank's solution. Then, they were made into 2 mL cell suspension, carefully dripped onto the surface of 2 mL rat lymphocyte isolator (Tianjin Haoyang Biological Products, China), and centrifuged (666 g) for 15 min. The rat lymphocytes on the interface were discarded, and the PMN was collected.

#### **Detection of Peripheral Blood PMN Apoptosis by Flow Cytometry**

The collected PMN was suspended with (Roswell Park Memorial Institute-1640) (RPMI-1640) medium (Wuhan Yipu Biotechnology, China). The density of cells was manually set to 1 $\times$ 10<sup>6</sup>/mL. Then, cells were placed in the culture plate and incubated in a CO<sub>2</sub> incubator (Guangzhou Haohan Instrument, China) for 6 h. The PMN suspension was placed in a centrifuge tube, washed with Phosphate Buffer Saline (PBS, Tianjin Guangcheng Chemical Reagent, China), and centrifuged (167 g) for 8 min. The supernatant liquid was disposed of. Then, PMN was added with 250  $\mu$ L binding buffer to resuspend the cells; 100  $\mu$ L cell suspension was pipetted into a 5 mL flow tube, added with 5  $\mu$ L Annexin V-FITC and 10  $\mu$ L propidium iodide labeling solution, mixed evenly, and incubated for 10 min in a light-proof environment at ordinary

temperature. The incubated PMN was added with 500 μL PBS. The apoptosis of PMN was assessed by flow cytometry (Beckman Coulter, USA), and the percentages of various cells were analyzed.

#### **Detection of PMN Total NF-κB p65 and Phospho-NF-κB p65 (p-NF-κB p65) Expressions by Western Blot**

The separated PMN was washed twice with PBS. The cell pellet was collected in a centrifuge tube, placed on the ice for 15 min, and vigorously flicked with fingers. Then, it was added with 250 μL lysis solution and flicked with fingers to lyse until no obvious pellet was seen. Then, cells were centrifuged, and the supernatant was collected. The bicinchoninic acid (BCA) method was utilized to detect the protein density of the sample. The remaining samples were stored at -70 °C. As per the molecular weight of the protein samples, the electrophoresis gels were primed. The samples were loaded, and the electrophoresis was performed. The polyvinylidene fluoride (PVDF) membrane was chosen and transferred in Bio-Rad membrane-transferring device. Then, it was taken out and washed 2×10 min with Tris-Buffered Saline and Tween 20 (TBST) (Shanghai Youyu Biotechnology, China). The washed membrane was blocked by 5% skimmed milk on a shaker (70 r/min, ordinary temperature) for 1.5 h; then, it was washed thrice by TBST, with 10 min for each time. Added with p65 antibody, phosphorylated p65 antibody, and internal reference β-actin antibody dilution, it was incubated on a shaker (70 r/min, 4°C) overnight and washed by TBST for 3×10 min. Afterward, it was added with the diluent of anti-antibody, incubated on a shaker (70 r/min, ordinary temperature) for 1.5 h, and washed by TBST for 3×10 min. The washed PVDF membrane was then put in Nitro-Blue-Tetrazolium/5-bromo-4-chloro-3-indolyl-phosphate (NBT/BCIP) developing solution and incubated at an ordinary temperature in a light-proof environment for 5-30 min or more until the bands were clear. Then, the membrane was washed with distilled water, dried at ordinary temperature, and scanned. The ImageJ software was utilized to analyze and determine the gray value of the NF-κB p65 protein band on the image analyzer. The gray value proportion of p-NF-κB p65 to NF-κB p65 indicated the activation level of the target protein NF-κB p65.

#### **Detection of SNHG11 mRNA Expression in Pulmonary Tissue by RT-PCR**

The total RNA of pulmonary tissue was extracted by the Trizol method, and a reverse transcription reaction was performed after quality inspection. The reaction solution was primed as per the succeeding components: 5 μg total RNA, 1 μL 50 μM Oligo (dT), and 1 μL 10 mM dNTP Mix; the RNase free water was added to make up the total volume to 10 μL. The sample was mixed by shaking, centrifuged briefly, reacted at 65 °C for 5 min, and placed on the ice. The reaction solution was primed as per the succeeding components: 4 μL 25 mM MgCl<sub>2</sub>, 2 μL 0.1M DTT, 2 μL 10×RT buffer, 1 μL SuperScript III-RT, and 1 μL RNaseOUT. The solution was then added with 10 μL of the primed cDNA synthesis solution, mixed by shaking and centrifuge briefly; next, it was allowed to react for 50 min at 50 °C, 10 min at 25 °C, 50 min at 50 °C, and 5 min at 85 °C. Finally, it was placed on the ice. The sample was slightly stirred to mix evenly, centrifuged briefly, added with 1 μL Rnase H, and reacted for 20 min at 37 °C. Thus, the synthesis of the first strand of cDNA was completed, which was utilized as a template for the PCR reaction. The reaction solution was primed as per the succeeding components: 1 μL template DNA, 2 μL 10×Reaction Buffer, 0.4 μL 10 mM dNTPs, 0.4 μL 10 μM Reverse Primer, 0.4 μL 10 μM Forward Primer, and 0.2 μL Easy Taq; the distilled water was added to make up to a total volume of 20 μL. After pre-denaturation at 94°C for 3 min, the sample underwent denaturation at 94°C for 30 s; the said reaction was repeated for 40 cycles. Then, the samples underwent 30s-annealing at 60 °C and 30s-extension at 72 °C. ΔCt was utilized to calculate and the results were represented by the 2<sup>-ΔΔCT</sup> method.

#### **Statistical Analysis**

SPSS 26.0 was utilized for data analysis. The measurement data were written mean ± standard deviation ( $\bar{x} \pm s$ ). The pair comparisons between samples utilized t-test. The counted data were written incidence n (%). The comparison was tested by Chi-square ( $\chi^2$ ). The multivariate analysis utilized binomial Logistic multiple regression analysis. Statistical significance was determined when P < 0.05.

## Results and discussion

### Results of ABGT and Pulmonary Tissue W/D Ratio

The results of ABGT were shown in Figure 1. Compared to Group C, PaO<sub>2</sub>, PaCO<sub>2</sub> and PaO<sub>2</sub>/FiO<sub>2</sub> of Group E, Group I, and Group A dropped, which had significance in terms of statistical analysis (P <0.05). Compared to Group E, PaO<sub>2</sub>, PaCO<sub>2</sub> and PaO<sub>2</sub>/FiO<sub>2</sub> of Group I dropped, which had significance in terms of statistical analysis (P <0.05). Compared to Group E and Group I, PaO<sub>2</sub>, PaCO<sub>2</sub> and PaO<sub>2</sub>/FiO<sub>2</sub> of Group A boosted, which had significance in terms of statistical analysis (P <0.05).

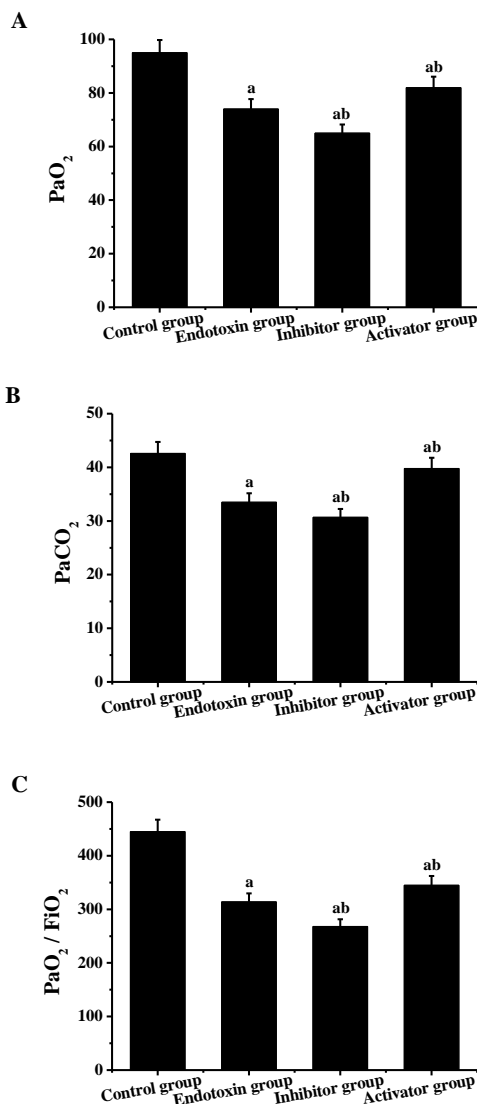


**Figure 1.** ABGT results (a: compared to Group C, P <0.05; b: compared to Group E, P <0.05). A. PaO<sub>2</sub>. B. PaCO<sub>2</sub>. C. PaO<sub>2</sub>/FiO<sub>2</sub>

The results of the pulmonary tissue W/D ratio were shown in Figure 2. Compared to Group C, the W/D

ratio of Group E, Group I, and Group A boosted, which had significance in terms of statistical analysis (P <0.05). Compared to Group E, the W/D ratio of Group I boosted, which had significance in terms of statistical analysis (P <0.05). Compared to Group E and Group I, the W/D ratio of Group A dropped, which had significance in terms of statistical analysis (P <0.05).

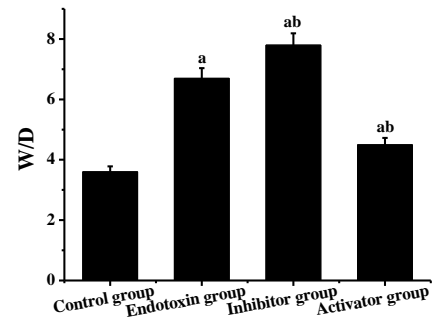


**Figure 2.** Results of pulmonary tissue W/D ratio (a: compared to Group C, P <0.05; b: compared to Group E, P <0.05)

### Results of HE Staining

The results of the pathological variations in the pulmonary tissues of the rats were shown in Figure 3. The pulmonary tissues of Group C were intact, without obvious pathological variations such as edema and inflammation. The lung interstitial of Group E and Group I showed obvious turbidity and swelling, with an increase in alveolar macrophages and lymphocytes, accompanied by infiltration of many neutral WBCs; in addition, some alveoli expanded, with a small amount of bleeding and edema in the alveolar cavity. Compared to Group E and Group I, the alveolar structure of Group A was more uniform and complete; besides, the turbidity and swelling of the interstitial lung, the inflammatory exudation in the alveoli, and the inflammatory cell infiltration were all reduced.

The results of the pathological scoring were shown in Figure 4. Compared to Group C, the pathological scores of Group E, Group I, and Group A boosted, which had significance in terms of statistical analysis (P <0.05). Compared to Group E, the pathological score of Group I was boosted, which had significance in terms of statistical analysis (P <0.05). Compared to Group E and Group I, the pathology score of Group A

dropped, which had significance in terms of statistical analysis ( $P < 0.05$ ).

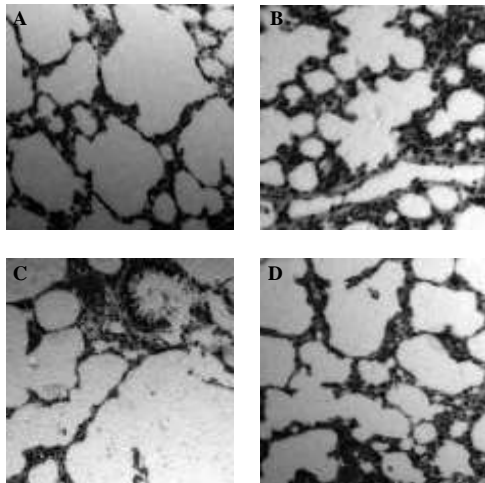


**Figure 3.** Pathological variations in pulmonary tissues A. Group C. B. Group E. C. Group I. D. Group A.

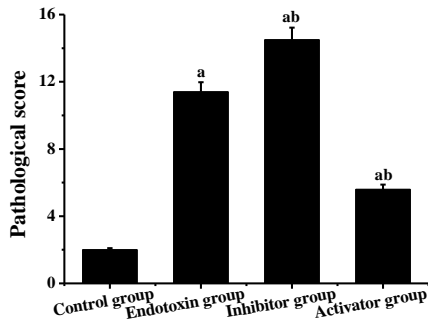


**Figure 4.** Results of pathological scores (a: compared to Group C,  $P < 0.05$ ; b: compared to Group E,  $P < 0.05$ )

### Results of flow Cytometry

The results of flow cytometry were shown in Figure 5. Compared to Group C, the PMN apoptosis rates of Group E, Group I, and Group A dropped, which had significance in terms of statistical analysis ( $P < 0.05$ ). Compared to Group E, the PMN apoptosis rate of Group I dropped, which had significance in terms of statistical analysis ( $P < 0.05$ ). Compared to Group E and Group I, the PMN apoptosis rate of Group A boosted, which had significance in terms of statistical analysis ( $P < 0.05$ ).

### Results of Western Blot

The results of Western Blot were shown in Figure 6. Compared to Group C, the expressions of p-NF-κB p65 in Group E, Group I, and Group A boosted, which had significance in terms of statistical analysis ( $P < 0.05$ ). Compared to Group E, the expression of p-NF-κB p65 in Group I was boosted, which had

significance in terms of statistical analysis ( $P < 0.05$ ). Compared to Group E and Group I, the p-NF-κB p65 expression of Group A dropped, which had significance in terms of statistical analysis ( $P < 0.05$ ). However, the expression of total NF-κB p65 between Groups was without statistical significance ( $P > 0.05$ ).

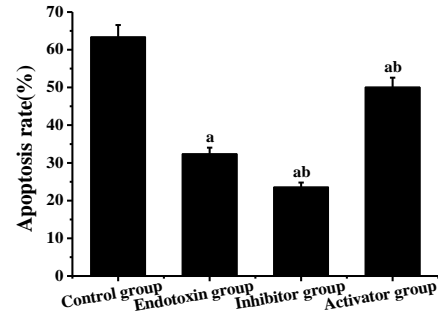


**Figure 5.** Results of flow cytometry (a: compared to Group C,  $P < 0.05$ ; b: compared to Group E,  $P < 0.05$ )

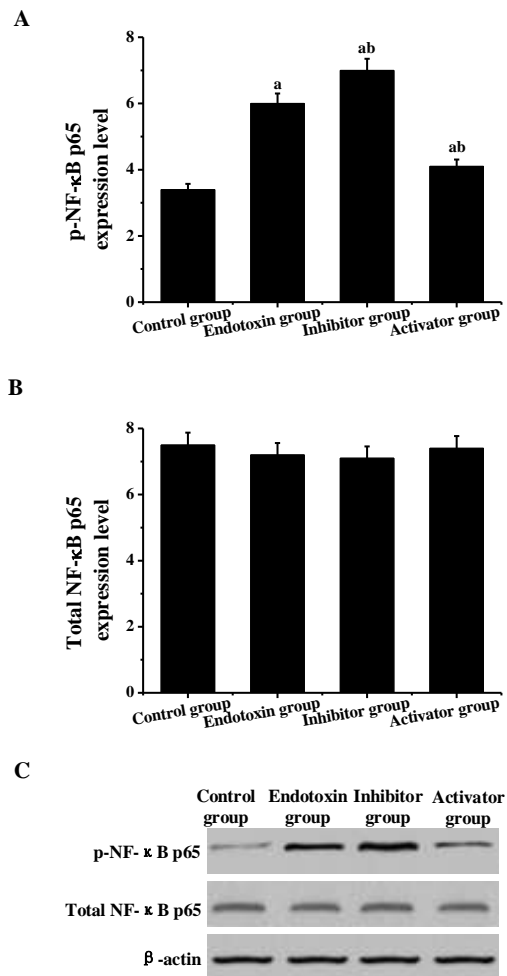


**Figure 6.** Results of western blot (a: compared to Group C,  $P < 0.05$ ; b: compared to Group E,  $P < 0.05$ ). A. p-NF-κB p65 expression. B. total NF-κB p65 expression. C. western blots protein bands

## Results of RT-PCR

The results of RT-PCR were shown in Figure 7. Compared to Group C, the expressions of SNHG11 mRNA in Group E, Group I, and Group A boosted, which had significance in terms of statistical analysis ( $P < 0.05$ ). Compared to Group E, the SNHG11 mRNA expression in Group I was boosted, which had significance in terms of statistical analysis ( $P < 0.05$ ). Compared to Group E and Group I, the SNHG11 mRNA expression in Group A dropped, which had significance in terms of statistical analysis ( $P < 0.05$ ).

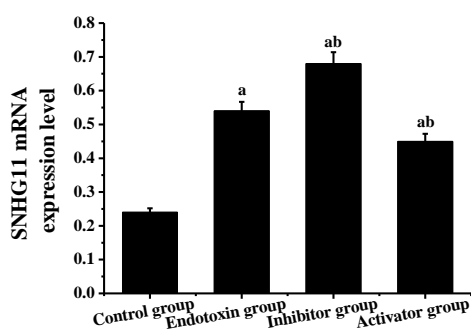


**Figure 7.** Results of RT-PCR (a: compared to Group C,  $P < 0.05$ ; b: compared to Group E,  $P < 0.05$ )

Essentially, ALI is diffuse alveolar-capillary membrane injury, which is mainly characterized by hypoxic respiratory insufficiency and massive inflammatory cell infiltration in pulmonary tissue. The massive inflammatory cell infiltration will increase capillary permeability, resulting in non-cardiogenic pulmonary edema; furthermore, as it develops, acute respiratory distress syndrome (ARDS) may occur (10). According to reports, ALI/ARDS can occur in all age groups; its incidence rate is about 18% to 38%, and its mortality rate is about 26% (11). The pathogenesis of ALI remained unclear. Therefore, the clinical treatment is not satisfactory. Scholars are earnest to find safer and more effective drugs for ALI treatments. Here, SD rats were utilized. The expressions of PMN total NF- $\kappa$ B p65 and p-NF- $\kappa$ B p65 were assessed by Western Blot, and the expression of SNHG11 mRNA in pulmonary tissue was assessed. The results showed that compared to Group C, the expressions of p-NF- $\kappa$ B p65 in Group E, Group I, and Group A boosted notably ( $P < 0.05$ ). Compared to Group E, the expression of p-NF- $\kappa$ B p65 in Group I boosted notably ( $P < 0.05$ ). Compared to

Group E and Group I, the p-NF- $\kappa$ B p65 expression of Group A dropped notably ( $P < 0.05$ ). However, the expression of total NF- $\kappa$ B p65 between Groups was without statistical significance ( $P > 0.05$ ). This showed that SNHG11 could slow the progression of ALI by inhibiting the activity of the NF- $\kappa$ B pathway. Research by Mathur and Vaishnav (2019) showed that SNHG11 could down-regulate the level of NF- $\kappa$ B in kidney tissue after ischemia-reperfusion injury in rat limbs (12). This was consistent with the results of this experiment.

Many studies have shown that once ALI occurs, PMN oozes into the pulmonary tissue, and there is a delay in apoptosis (13-15). Theoretically, PMN apoptosis is inhibited, which promotes PMN necrosis and the further development of ALI; in addition, the boosted PMN survival will lead to prolonged PMN alveolitis (16). Therefore, proper removal of PMN and its harmful contents will help control inflammation. Here, the impacts of SNHG11 on endotoxin-induced PMN apoptosis in ALI rats were explored. The results showed that compared to Group C, the PMN apoptosis rates of Group E, Group I, and Group A dropped notably ( $P < 0.05$ ). Compared to Group E, the PMN apoptosis rate of Group I dropped notably ( $P < 0.05$ ). Compared to Group E and Group I, the PMN apoptosis rate of Group A boosted notably ( $P < 0.05$ ). Lee et al. (2017) believed that PMN could play a role in the LPS-induced ALI by affecting the activation of NF- $\kappa$ B (17-19). This was consistent with the results of this experiment.

In summary, SNHG11 could reduce endotoxin-induced ALI by promoting PMN apoptosis and inhibiting the NF- $\kappa$ B pathway. The results provided a reference for the clinical prevention and treatment of ALI, which had great worth. However, limitations were inevitable in the experimental process. For instance, the sample size was small, which might lead to biased results. Therefore, more samples would be included in the following experiments to perfect the results.

## Acknowledgments

Taizhou Science and Technology Bureau, Effect and Mechanism of Free Ubiquitin in Acute Lung Injury (No. 1801ky21).

## Conflict interest

None.

## References

1. Ma C, Long H, Yang C, Cai W, Zhang T, Zhao W. Anti-inflammatory role of pilose antler peptide in LPS-induced lung injury. *Inflamm* 2017;40(3):904-12.
2. Jambrovics K, Uray IP, Keresztesy Z, Keillor JW, Fésüs L, Balajthy Z. Transglutaminase 2 programs differentiating acute promyelocytic leukemia cells in all-trans retinoic acid treatment to inflammatory stage through NF- $\kappa$ B activation. *haematol* 2019;104(3):505.
3. Li W, Zhao R, Wang X, Liu F, Zhao J, Yao Q, Zhi W, He Z, Niu X. Nobilentin-ameliorated lipopolysaccharide-induced inflammation in acute lung injury by suppression of NF- $\kappa$ B pathway in vivo and vitro. *Inflamm* 2018;41(3):996-1007.
4. Lv H, Yu Z, Zheng Y, Wang L, Qin X, Cheng G, Ci X. Isovitexin exerts anti-inflammatory and antioxidant activities on lipopolysaccharide-induced acute lung injury by inhibiting MAPK and NF- $\kappa$ B and activating HO-1/Nrf2 pathways. *Intl J Biol Sci* 2016;12(1):72.
5. Zamoshnikova A, Groß CJ, Schuster S, Chen KW, Wilson A, Tacchini-Cottier F, Schroder K. NLRP12 is a neutrophil-specific, negative regulator of in vitro cell migration but does not modulate LPS-or infection-induced NF- $\kappa$ B or ERK signalling. *Immunobiol* 2016;221(2):341-6.
6. Luo Y, Pang XX, Ansari AR, Wu XT, Li HZ, Zhang ZW, Song H. Visfatin exerts immunotherapeutic effects in lipopolysaccharide-induced acute lung injury in murine model. *Inflamm* 2020;43(1):109-22.
7. Liu B, Chen Y, Yang J. LncRNAs are altered in lung squamous cell carcinoma and lung adenocarcinoma. *Oncotarget*. 2017;8(15):24275.
8. Xu W, Zhou G, Wang H, Liu Y, Chen B, Chen W, Lin C, Wu S, Gong A, Xu M. Circulating lncRNA SNHG11 as a novel biomarker for early diagnosis and prognosis of colorectal cancer. *Int J Cancer*. 2020;146(10):2901-12.
9. Zhao Q, Fan C. A novel risk score system for assessment of ovarian cancer based on co-expression network analysis and expression level of five lncRNAs. *BMC Medical Genet* 2019 ;20(1):1-3.
10. Cadirci E, Ugan RA, Dincer B, Gundogdu B, Cinar I, Akpınar E, Halici Z. Urotensin receptors as a new target for CLP induced septic lung injury in mice. *Naunyn Schmiedebergs Arch Pharmacol* 2019;392(2):135-45.
11. Gao Y, Lv X, Yang H, Peng L, Ci X. Isoliquiritigenin exerts antioxidative and anti-inflammatory effects via activating the KEAP-1/Nrf2 pathway and inhibiting the NF- $\kappa$ B and NLRP3 pathways in carrageenan-induced pleurisy. *Food Funct* 2020;11(3):2522-34.
12. Mathur P, Vaishnav S. Pathophysiology of acute kidney injury in severe acute pancreatitis-an overview. *Gastroenterol Hepatol* 2019;10:242-5.
13. Chi X, Guo N, Yao W, Jin Y, Gao W, Cai J, Hei Z. Induction of heme oxygenase-1 by hemin protects lung against orthotopic autologous liver transplantation-induced acute lung injury in rats. *J Transl Med* 2016;14(1):1-9.
14. Sun LC, Zhang HB, Gu CD, Guo SD, Li G, Lian R, Yao Y, Zhang GQ. Protective effect of acacetin on sepsis-induced acute lung injury via its anti-inflammatory and antioxidative activity. *Archi Pharma Res* 2018;41(12):1199-210.
15. Wu H, Zhao G, Jiang K, Li C, Qiu C, Deng G. Engeletin alleviates lipopolysaccharide-induced endometritis in mice by inhibiting TLR4-mediated NF- $\kappa$ B activation. *J Agric Food Chem* 2016;64(31):6171-8.
16. Davino-Chiovatto JE, Oliveira-Junior MC, MacKenzie B, Santos-Dias A, Almeida-Oliveira AR, Aquino-Junior JC, Brito AA, Rigonato-Oliveira NC, Damaceno-Rodrigues NR, Oliveira AP, Silva AP. Montelukast, leukotriene inhibitor, reduces LPS-induced acute lung inflammation and human neutrophil activation. *Archivos de Bronconeumología (English Edition)*. 2019;55(11):573-80.
17. Bakhshi, B. Heat and Drought Stress Response and Related Management Strategies in Oilseed Rape. *Agrotech Ind Crops* 2021; 1(4): 170-181. doi: 10.22126/atic.2022.7239.1034
18. Lee JM, Yeo CD, Lee HY, Rhee CK, Kim IK, Lee DG, Lee SH, Kim JW. Inhibition of neutrophil elastase contributes to attenuation of lipopolysaccharide-induced acute lung injury during neutropenia recovery in mice. *J Anesth* 2017;31(3):397-404.
19. Behzadmehr R, Rezaie-Keikhaie K. Evaluation of Active Pulmonary Tuberculosis Among Women With Diabetes. *Cellular, Molecular and Biomedical Reports*, 2022, 2(1):56-63. doi:10.55705/cmbr.2022.336572.1036